INSTITUTE OF PHYSICS PUBLISHING MEASUREMENT SCIENCE AND TECHNOLOGY

Meas. Sci. Technol. **16** (2005) 1903–1912 doi:10.1088/0957-0233/16/10/004

Large-scale laboratory observations of turbulence on a fixed barred beach

Christopher P Scott, Daniel T Cox, Timothy B Maddux and Joseph W Long

O H Hinsdale Wave Research Laboratory, Oregon State University, Corvallis, OR 97331-2302, USA

E-mail: scottc2@engr.orst.edu

Received 12 January 2005, in final form 8 April 2005
Published 23 August 2005
Online at stacks.iop.org/MST/16/1903

Abstract

The details of a large-scale laboratory experiment to study the turbulence generated by waves breaking on a fixed barred beach are presented. The data set includes comprehensive measurements of free surface displacement and fluid velocity for one random and one regular wave case. Observations of the time-averaged turbulent kinetic energy per unit mass, $\overline{k}$, show that the turbulence generated by wave breaking was greatest at the bar crest and did not fully dissipate prior to reaching the bed. This indicates that, even in a time-averaged sense, wave breaking turbulence may be important for near-bed processes. Onshore of the bar, turbulence was generally confined to the upper part of the water column and had dissipated once the waves reformed (approximately 1.5 wavelengths onshore of the bar crest). The turbulent structure was the same in the random and regular wave cases; however, the magnitude of $\overline{k}$ was much less in the random wave case, despite similar offshore wave conditions. Additionally, three methods were used to separate the wave-induced and turbulent components of velocity: ensemble averaging, high-pass filtering and a differencing method proposed by Trowbridge (1998 *J. Atmos. Ocean. Technol.* **15** 290–8). The magnitude of $\overline{k}$ varied by as much as a factor of 5 among these methods, but qualitatively, the cross-shore and vertical structure were independent of the method used. The differencing method agreed closely with ensemble averaging in terms of the magnitude and structure of time-averaged quantities and in the signature of the time-dependent turbulent kinetic energy. Given this agreement, the differencing method appears to be the most suitable for application to random waves, such as those observed in the field.

Keywords: turbulence, breaking waves, laboratory experiment, surf zone, barred beach

1. Introduction

In the surf zone, wave energy is transformed into turbulent energy through breaking. The turbulence generated by wave breaking can dominate surf zone flows (Trowbridge and Elgar 2001) and processes of sediment suspension (Fredsøe and Deigaard 1992). Furthermore, the difficulty in making direct observations of surf zone turbulence has hindered our ability to adequately quantify and predict sediment transport. Prototype-scale laboratory experiments have been suggested as a facilitator for improved understanding of the processes of breaking waves and their associated turbulence (Thornton *et al* 2000).

Prototype-scale laboratory experiments are necessary because many of the existing studies on wave breaking turbulence have been conducted in small-scale laboratory flumes (e.g., Stive (1980), Nadaoka and Kondoh (1982), Ting and Kirby (1994), Cox *et al* (1995)) and scaling issues may arise when extrapolating hydrodynamic quantities, such as the vertical variation of horizontal turbulence intensity, to

field conditions. Additionally, most of these experiments were conducted using planar beaches, and only recently has attention been given to complex bathymetries such as a barred beach (e.g., Sancho *et al* (2001)), despite the numerous modelling efforts for predicting field-observed bar motions (e.g., Hoefel and Elgar (2003)). In the laboratory, repeatable wave conditions and the use of a fixed bed provide a unique opportunity to collect a detailed, synoptic data set without the influence of three-dimensional wave and current fields, tides, and wind. It also allows the use of sensitive instrumentation likely to be damaged in a field deployment.

The objective of this experiment is to provide a large-scale, synoptic picture of the time-averaged turbulent kinetic energy in the nearshore, and to determine whether the turbulence from wave breaking is transported to the bed on a barred profile. Additionally, we compare three methods of separating turbulent and wave-induced fluid velocity components to determine whether the method used affects the magnitude or spatial structure of the turbulence estimates. Section 2 briefly describes these three methods, followed by the experimental setup and post-processing of the data in sections 3 and 4, respectively. Section 5 outlines the application of each method to the data and section 6 compares the turbulence estimates from all three. Observations of the cross-shore and vertical structure of the turbulence generated over the bar are presented in section 7, followed by the main conclusions in section 8.

2. Methods of separating wave and turbulent motions

In the nearshore, the observed fluid velocity (u) can be decomposed into mean, wave-induced and turbulent components as follows:

$$u = \bar{u} + \tilde{u} + u' \tag{1}$$

where an overbar denotes time-averaged (mean) quantities, a tilde denotes wave-induced quantities and a prime denotes turbulent quantities. Separating the wave-induced and turbulent components is difficult and several methods are suggested in the literature. Svendsen (1987) reviewed three of these methods and compared scaled measurements of the time-averaged turbulent kinetic energy per unit mass ($\overline{k}$) obtained from the laboratory experiments of Stive and Wind (1982), Nadaoka and Kondoh (1982) and Hattori and Aono (1985), where $\overline{k}$ is defined as

$$\overline{k} = \tfrac{1}{2}(\overline{u'u'} + \overline{v'v'} + \overline{w'w'}) \tag{2}$$

where u, v and w are the cross-shore, alongshore and vertical velocities, respectively. Despite the different methods used to separate the turbulent signal, Svendsen (1987) observed that characteristic features, such as a weak variation of $\overline{k}$ over depth, were consistent for all the measurements when scaled using the squared shallow water wave speed. In our work, three separation methods are applied to the two data sets collected. This allows for a direct comparison of the turbulent quantities and eliminates errors that may arise when scaling the results obtained from different experiments. In addition to comparing two of the methods reviewed by Svendsen (1987), ensemble averaging and high-pass filtering, we add a third technique proposed by Trowbridge (1998).

2.1. Ensemble averaging

When regular waves are studied, the wave-induced velocity can be estimated by averaging the same point in the wave phase over many successive waves (ensemble averaging) and the turbulent component can then be estimated using equation (1). This method has been used extensively in the literature (e.g., Stive and Wind (1982), Ting and Kirby (1994) and Cox *et al* (1995)) and Svendsen (1987) concluded that it must be considered the only well-defined way of separating wave and turbulent motions when discussing regular waves. It also has the advantage of allowing large, low-frequency vortices, typically neglected by other methods, to be recorded as turbulence, provided they are not identically repeated wave to wave. An obvious limitation of this method is that it cannot be applied to truly random waves in the field. However, in the laboratory this method can be applied to random waves by collecting many realizations of the same velocity time series at a single location and averaging these realizations to obtain the wave-induced velocity.

2.2. High-pass filtering

When waves are not repeatable, high-pass filtering can be used to separate the wave-induced and turbulent components of velocity by specifying a cutoff frequency separating the wave and turbulent time scales, then applying standard filtering techniques to isolate the high-frequency (turbulent) component. Choosing an appropriate cutoff frequency can be difficult, and it is possible that a single cutoff separating these scales is physically unattainable (Nadaoka *et al* 1989). Depending on the cutoff frequency chosen, this method may neglect large-scale vortices produced by breaking that are of a lower frequency than the higher harmonics of the organized wave motion. In fact, Svendsen (1987) observed that scaled turbulence estimates obtained using the high-pass filtering method were generally smaller than those obtained using ensemble averaging.

2.3. Differencing

Trowbridge (1998) proposed a technique that utilizes the difference between the measured velocities (Δu) from two closely spaced sensors to estimate the average turbulent velocity variance and covariance between the sensors. For example, the turbulent velocity variance in the cross-shore direction ($\overline{u'u'}$) can be estimated as follows:

$$\langle \overline{u'u'} \rangle = \tfrac{1}{2}\,\mathrm{var}(\Delta u) \tag{3}$$

where $\langle\,\rangle$ is used to denote a spatial average between the sensors, u is the total velocity and $\Delta u = u_1 - u_2$, where u_1 and u_2 are the observed total velocities from each of the two sensors. This method can be applied to random waves and requires that the sensors be separated such that the wave component of velocity is correlated and the turbulent component is uncorrelated between the two sensors. In general terms, this means that the separation distance between the sensors must be slightly larger than the largest eddy produced by wave breaking. In addition, this separation should be perpendicular to the direction of wave propagation (i.e. parallel to the wave crests), which causes errors when the seas are multidirectional.

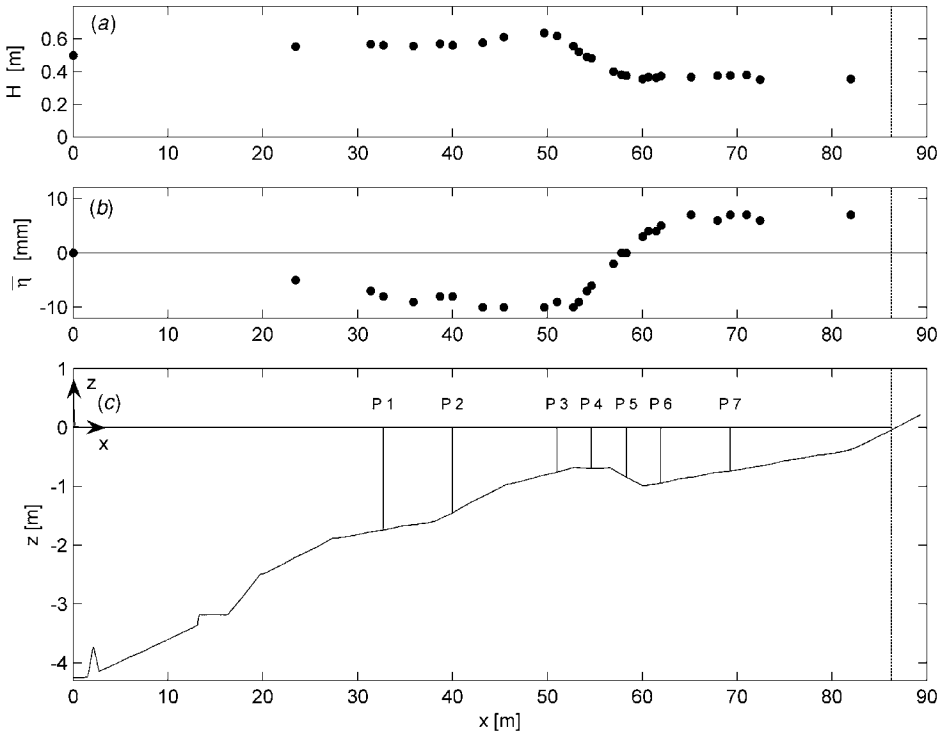

Figure 1. Cross-shore variation of H (a) and $\bar{\eta}$ (b) for the random wave case. Surveyed bathymetry and locations of velocity profiles P1–P7 (c). Wavemaker located at $x = 0$, still water shoreline indicated by (- - -).

3. Experimental setup

3.1. Large wave flume and barred profile

The experiment was conducted in the large wave flume at Oregon State University's O H Hinsdale Wave Research Laboratory. The basin is 104 m long, 3.7 m wide, and 4.6 m deep with a programmable flap-type wavemaker equipped with active wave absorption and maximum wave capability of $H = 1.6$ m at $T = 3.5$ s. For this project, a model beach was constructed by fixing concrete slabs to the sidewalls of the flume, resulting in the piecewise continuous profile shown in figure 1(c). The model bathymetry approximated the bar geometry for the average profile observed on 11 October 1994, of the DUCK94 field experiment (e.g., Garcez Faria *et al* (2000)) at a 1:3 scale. The model was compressed in the cross-shore relative to field-observed bars due to the limitation of the flume length. Nevertheless, it captured the hydrodynamic processes of wave breaking and reforming common to natural barred beaches. The friction factor, f_w, was estimated using the semitheoretical expression developed by Jonsson (1966) for rough turbulent flow:

$$\frac{1}{4\sqrt{f_w}} + \log\left(\frac{1}{4\sqrt{f_w}}\right) = \log\left(\frac{A_b}{k_s}\right) - 0.08 \qquad (4)$$

where A_b is the excursion amplitude at the bed estimated using linear wave theory and k_s is the Nikuradse sand roughness typically estimated using the grain diameter ($k_s = 2d_{50}$). Using an estimate range of 0.04 mm $< k_s <$ 0.2 mm and the breaking wave heights and periods listed in table 1 in a water depth of 0.80 m, estimates of the wave friction factor fell in the range of $0.005 < f_w < 0.007$. In comparison, applying the same approach to the average wave conditions from the 8 m array on 11 October 1994, at Duck, NC ($H_{mo} = 1.8$ m, $T_p = 6.6$ s, $h = 8.3$ m) with $d_{50} = 0.2$ mm yielded a friction factor of $f_w = 0.008$.

Table 1. Deep water and breaking wave conditions measured during the experiment.

	T (s)	H_0 (m)	L_0 (m)	H_b (m)	L_b (m)	ξ_b	t_{dur} (min)	N_{waves}
Random	4.0	0.59	25.0	0.64	10.9	0.35	20	342
Regular	4.0	0.64	25.0	0.75	10.9	0.32	10	150

3.2. Wave conditions and free surface measurements

In this study, a random time series approximating a narrow banded sea (TMA spectrum, $\gamma = 20$) was used to study the wave-breaking process under forcing similar to the field. Regular waves were also used to allow the ensemble averaging technique to be applied. In both cases, the target offshore wave height and period were scaled using the average significant wave height ($H_{mo} = 1.8$ m) and peak period ($T_p = 6.6$ s) observed at the 8 m array on 11 October 1994, of the DUCK94 field experiment. Active wave absorption was used for the regular wave case. It was not used for the random wave case because it limited the size of the waves that could be generated. Additionally, preliminary investigations using similar wave conditions and the underlying 1:36 planar beach indicated that active wave absorption did not significantly reduce energy at low frequencies for the random wave case.

Resistance-type wave gauges sampling at 50 Hz were used to measure the free surface elevation (η) at 28 locations in the basin. To validate the repeatability of the experiment, six

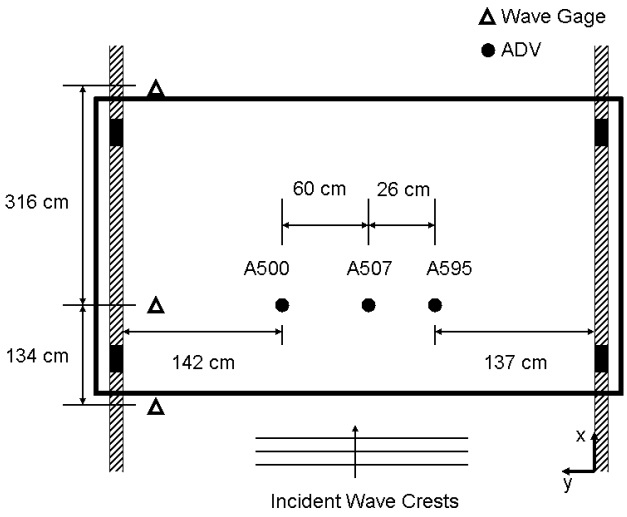

Figure 2. Plan view of the movable instrument cart with the locations of the ADV array and three wave gauges shown. All three ADVs were collocated in the vertical and cross-shore directions.

gauges remained fixed during the study ($x = 23.45$ m, 45.40 m, 52.73 m, 60.04 m, 70.99 m, 81.97 m) and one was mounted on the wavemaker ($x = 0.00$ m). Additionally, η was measured using three wave gauges mounted on a movable cart used for collecting velocity profiles, as shown in figure 2.

The deep water and breaking wave characteristics for the random and regular cases are listed in table 1. The subscripts $()_0$ and $()_b$ are used to denote deep water and breaking parameters, respectively. For the random wave case, T is the spectral peak period and H is the significant wave height calculated using zero upcrossing. For the regular wave case T and H are the ensemble-averaged wave period and wave height calculated using zero upcrossing. In both cases the deep water wave length (L_0) and wave height (H_0) were calculated using linear wave theory. The average slope on the offshore side of the bar ($\tan\alpha_b = 1/18$) was used to calculate the Iribarren number $\left(\xi_b = \frac{\tan\alpha_b}{\sqrt{H_b/L_0}}\right)$. It is noted that the values obtained for ξ_b are slightly below the plunging criterion $0.4 < \xi_b < 2.0$ suggested by Battjes (1974). However, the random waves were observed to be both plunging and spilling as far offshore as $x = 42$ m, and the regular waves were plunging at $x = 53$ m. Approximately $N = 342$ waves were recorded in the random wave case, which exceeds the minimum of 200 prescribed by Goda (2000) for a simulated sea state. For the regular wave case, $N = 150$ waves were used, exceeding the number used in previous studies (e.g., Ting and Kirby (1994): $N \cong 100$, Cox *et al* (1995): $N = 50$).

Figures 1(*a*) and (*b*) show the cross-shore variation of H and mean water level ($\bar{\eta}$) for the random wave case, clearly showing the shoaling ($x < 50$ m), breaking (50 m $< x <$ 60 m) and reforming ($x > 60$ m) regions. The measured variation in $\bar{\eta}$ was consistent with Bowen *et al* (1968) who found that the maximum set-down occurs slightly onshore of breaking.

3.3. Velocity measurements

Vertical profiles of velocity time series were recorded at seven cross-shore locations (P1–P7, figure 1(*c*)). Of primary interest were the profiles at the bar crest (P4), where wave breaking was most intense, and just onshore of the crest where wave breaking turbulence was carried onshore (P5 and P6). At each of the seven cross-shore locations, time series were recorded at eight vertical locations: 1 cm, 5 cm and 10 cm above the fixed bed, followed by five additional elevations evenly spaced between 10 cm above the bed and trough level.

At each vertical location, velocities were sampled synchronously at 50 Hz using three 3D, down-looking SonTek 16 MHz micro acoustic Doppler velocimeters (ADVs). The ADVs were collocated in the vertical and cross-shore, but separated in the alongshore (figure 2). The alongshore separation was designed to test whether each ADV observed the same wave-induced component of velocity when applying the differencing method. For the random waves, the spacing between the ADVs was 26 cm and 60 cm with the outermost ADVs 137 cm and 142 cm from the sidewalls. This allowed for as large a separation scale as possible while minimizing the effect of the sidewalls on the observed velocities. For the regular wave case, only two ADVs were used (A500 and A507) with a 60 cm alongshore spacing. The coordinate system, shown in figures 1(*c*) and 2, was x positive onshore, z positive up and y consistent with a right-hand coordinate system. The origin was located at the intersection of the wavemaker and the still water line.

To obtain a synoptic data set, the same 20 min random time series was run at each of the eight elevations for all seven profiles (56 total runs), and each run was synchronized with the start of wavemaker motion. Data for the regular wave case were collected in 60 min runs, during which time the velocity was measured at four elevations in the profile by recording at each elevation for 10 min. The first 5 min of each 60 min run were eliminated to allow the wave conditions to reach a steady state. The still water interval between each run was 20 min for both random and regular waves.

4. Data reduction

4.1. Free surface

All free surface data were reduced using ensemble averaging techniques. For the random wave case, this consisted of averaging 56 realizations of the 20 min time series for each of the seven fixed wave gauges, and eight realizations for the three wave gauges on the movable cart with the ADV array. For the regular wave case, approximately 8400 waves were averaged for each of the fixed wave gauges, and 1200 waves were averaged for the gauges on the cart. Seaward of breaking, the average standard deviation of the ensemble-averaged wave was less than 1.0 cm (1.5% of full scale) and 1.5 cm (2.4% of full scale) for the random and regular wave cases, respectively, verifying the repeatability of the wave conditions.

4.2. Velocity

All velocity time series were post-processed to address three sources of noise: signal dropouts and spikes, Doppler noise and instrument vibration. Signal dropouts due to instruments coming out of the water, and signal spikes caused by air bubbles or a lack of particulate matter within the flow are common when using ADVs in the surf zone (e.g., Elgar *et al* (2001)). In this test, valid measurements were defined as those

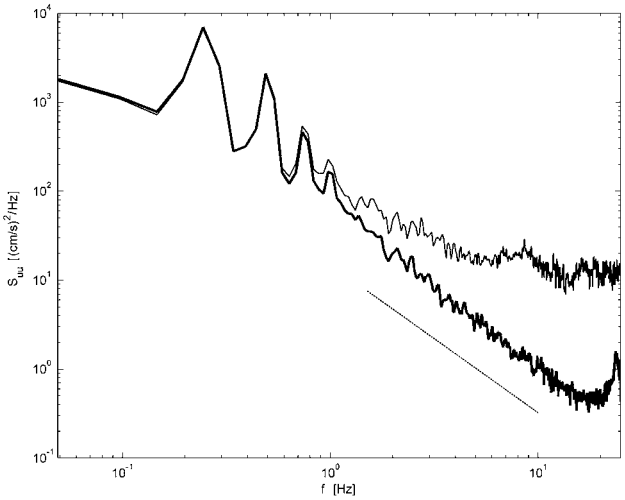

Figure 3. Typical raw (light) and despiked (heavy) cross-shore velocity spectra. Data are from the regular wave case P4, 34 cm above the bed. $-5/3$ slope added for reference (- - -).

having a signal-to-noise ratio (SNR) greater than 10 dB and correlation greater than 70%, where these quantities are the average values along all three ADV beams. Additionally, the phase-space-threshold criterion outlined by Goring and Nikora (2002) was used to identify spikes that were not identified by the SNR and correlation thresholds. After invalid samples were identified, a cubic spline between valid samples was used to replace them. The median percentage of the record identified as invalid was 2.3% and 2.7% for the random and regular wave cases, respectively, with significantly higher values (20–30%) near trough level at P4 and P5. Figure 3 shows the raw and despiked cross-shore velocity spectra for ADV A500 at P4, 34 cm above the bed. The $-5/3$ slope, characteristic of an inertial subrange, is biased high in the raw data at frequencies above 2–3 Hz. This is indicative of white noise in the data, and the energy associated with that high-frequency portion of the spectrum is typically referred to as the noise floor. It is clear that after removing signal dropouts and spikes, the noise floor was significantly reduced and more accurate estimates of the turbulent velocity variance were obtained.

Doppler noise, white noise present at all frequencies, is inherent in all coherent Doppler velocimeters and can significantly bias velocity variance estimates (Nikora and Goring 1998). After removing signal dropouts and spikes, the magnitude of the Doppler noise floor was estimated from the high-frequency portion of the spectrum and integrated over the frequency range used to estimate the variance. This yielded an estimate of the noise contribution to the variance, and was subtracted from the total variance prior to estimating turbulent quantities, such as $\overline{k}$.

Finally, velocity data were filtered to remove noise from high-frequency instrument vibration caused by breaking waves hitting the 40 cm stem on the ADVs and the supports used to deploy the ADVs in the flume. Noise due to vibration of the ADV stem was present in the u and v components of velocity and centred at 24 Hz, as shown in the despiked spectrum in figure 3. In the u component of velocity, a seventh order Chebyshev type II low-pass filter with a corner frequency of 20 Hz was used to remove this noise from the record. Vibration from the supports used to deploy the ADVs was only present in the v component of velocity and occurred at frequencies between 12 and 20 Hz. A sixth order filter of the same type with a cutoff frequency of 10 Hz was used to remove this noise along with the noise from the ADV stem vibration from v. The w component of velocity was unaffected by any vibration and was not filtered.

Accounting for these sources of noise significantly reduced estimates of $\overline{k}$ for both the random and regular wave cases. The average per cent reduction in $\overline{k}$ for all of the measurements was 27%, 52% and 22% for the ensemble averaging, high-pass filtering and differencing methods, respectively.

5. Application of the turbulence separation methods

Each of the three methods described in section 2 was applied to the post-processed data using the following procedures. The ensemble averaging technique was applied to the regular wave case by separating individual waves using a zero-upcrossing technique, scaling the wave period to $T = 4.0$ s, then computing the wave component of velocity. This was to ensure that the velocity was averaged relative to the same point in the wave phase because the wave period in the surf zone varies slightly, even when running regular waves (Svendsen 1987). Additionally, low-frequency fluctuations in the velocity that would have been recorded as turbulent velocities 'pseudo-turbulence' were removed by high-pass filtering the raw signal at 0.0625 Hz (one-quarter of the peak wave frequency) prior to ensemble averaging. After calculating the wave component of velocity, the turbulent component was estimated by subtracting the wave component from the total velocity between the zero crossings used to separate each wave. The ensemble averaging technique was also applied to one elevation of the random wave case by repeating the same random time series seven times at P5 with all three ADVs 32 cm above the bed (21 realizations). In this case, each time series was treated as a 'wave' and the procedure described above was applied.

The high-pass filter selected to isolate turbulent motions from wave-induced motions was a seventh order Chebyshev type II filter with a cutoff frequency of 1 Hz. This cutoff was chosen based on visual inspection of the low-frequency end of the $-5/3$ slope in the power spectral density of the observed cross-shore velocity. A cutoff of 1 Hz also corresponds to four times the peak wave frequency, and is lower than the cutoff of Nadaoka *et al* (1989) who used approximately seven times the peak wave frequency. The results obtained using this method are highly sensitive to the cutoff chosen and it was found that increasing it by a factor of 2 reduced the magnitude of $\overline{k}$ by 40% in both the random and regular wave cases.

As described earlier, the method of Trowbridge (1998) requires that the waves be unidirectional. This assumption was valid offshore (P1–P3) and for the breaking region over the bar crest (P4–P6) in the random and regular wave cases. However, during regular wave runs, the waves were not alongshore uniform in the inner surf zone (P7). This alongshore partial standing wave was not observed for waves with longer periods ($T = 7$ s) that would break continuously from the bar crest to the shoreline, or for waves with shorter periods ($T = 2$ s)

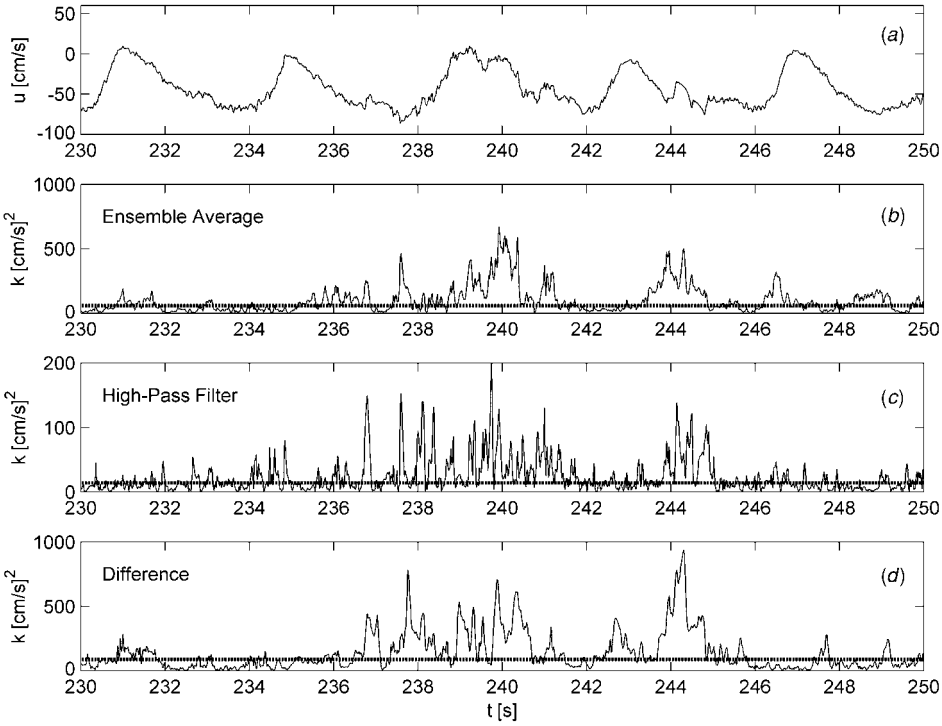

Figure 4. Time variation of u (a) and k from the ensemble averaging (b), high-pass filtering (c) and differencing methods (d). Average k for the time series indicated by (- - -). Data are from the regular wave case, P5, 10.4 cm above the bed, using ADV A500 for (a)–(c) and A500 and A507 for (d).

that would quickly reform after breaking on the bar. Due to these alongshore inhomogeneities in the inner surf zone, differencing estimates should be treated with caution at P7, and it is noted that all three methods estimated little turbulent kinetic energy at this location.

6. Comparison of turbulence separation methods

To illustrate the application of each method to a typical time series, figure 4 shows the temporal variation of u and k, where k is the time-dependent turbulent kinetic energy per unit mass. Data are from the regular wave case at P5, 10.4 cm above the bed. In this figure, the ensemble averaging and high-pass filtering methods were applied to ADV A500 and the differencing method was applied to A500 and A507. It is noted that the ensemble averaging and high-pass filtering methods estimated k at a single location, whereas the differencing method estimated the average value of k between the two sensors. The time-averaged value of k for the entire time series, equal to $\overline{k}$ for the ADVs used, is also shown with a horizontal dashed line. In this figure we see that the magnitude of k was similar where the ensemble averaging and differencing methods were applied, and both were about five times larger than the values from high-pass filtering (note the change in y-axis scale). Furthermore, despite the regular forcing, all three methods exhibited an intermittent nature, whereby the instantaneous value of k was an order of magnitude larger than the average value, as observed by Cox and Kobayashi (2000). The signatures from the ensemble averaging and differencing methods were qualitatively similar and made up of a few large events, whereas the signature from high-pass filtering contained many more short events. This difference is attributed to the fact that the high-pass filtered data only contained energy at frequencies greater than 1 Hz. A detailed study of the intermittent properties is left for future work.

To provide a synoptic picture of how the separation method affected the magnitude and spatial structure of the turbulence, estimates of $\overline{k}$ from each method were compared. For the random wave case, $\overline{k}$ was estimated independently using each ADV, and the value reported herein is the average of the three. The same procedure was followed for the regular wave case, but only ADVs A500 and A507 were used because of problems with the synchronization of A595. It is important to note that it is impossible to compare the results of each method to the true value; therefore, we can only indicate whether each method consistently provides a low/high estimate and assume that the true value lies somewhere among the three.

Figure 5 shows the vertical variation of $\overline{k}$ estimated using all three methods at P4–P6 for the random and regular wave cases. In both cases the high-pass filter provided a low estimate of $\overline{k}$, despite the fact that a lower cutoff than Nadaoka *et al* (1989) was used. This was most likely due to energy neglected from large eddies with frequencies lower than 1 Hz, and is consistent with the comparisons made by Svendsen (1987). In the regular wave case, $\overline{k}$ estimates from the differencing method were approximately 26% larger than the ensemble-averaging values. If ensemble averaging is considered to be a well-defined way to separate wave-induced and turbulent motions for regular waves, then these results indicate that the differencing method can be used to reasonably estimate $\overline{k}$ in the presence of regular waves. This can be extended to random waves as well, because this method does not require

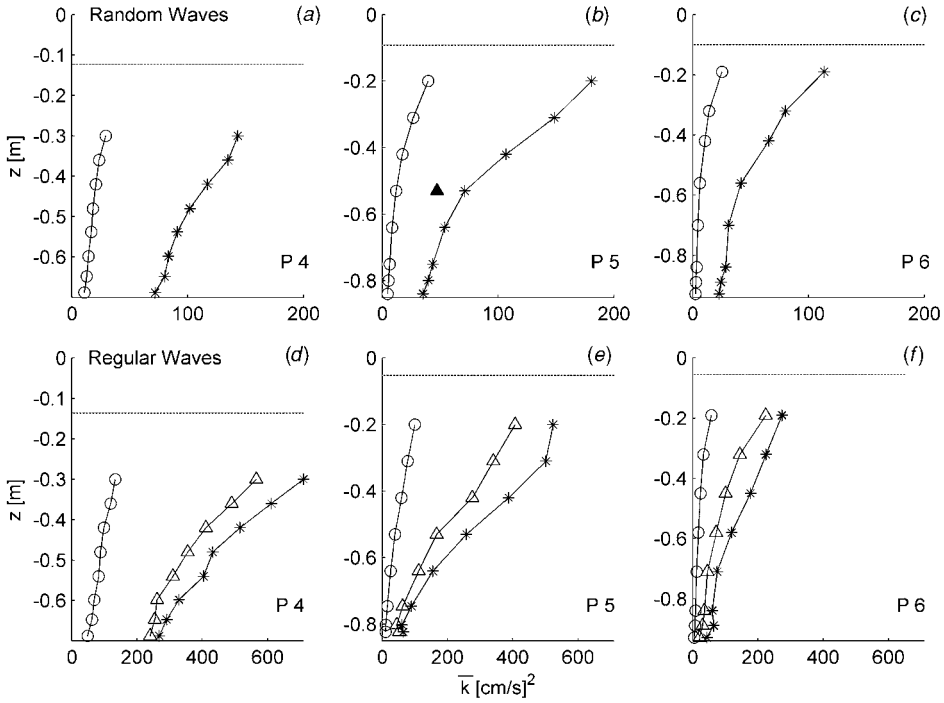

Figure 5. Vertical variation of $\overline{k}$ for random (*a*)–(*c*) and regular (*d*)–(*f*) waves at P4–P6 using ensemble averaging (△), high-pass filtering (○) and differencing (∗) techniques. Ensemble averaging estimate from the repeated random wave runs included at P5 (▲). Trough level indicated by (- - -), bottom of the figure indicates the fixed bed.

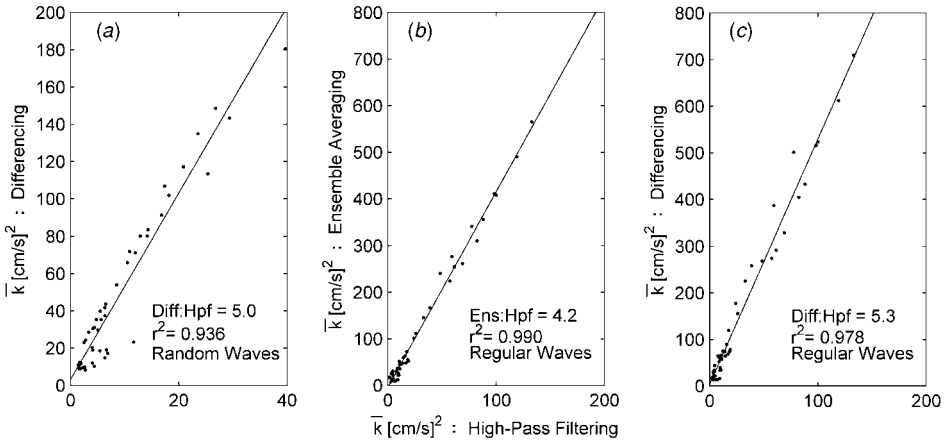

Figure 6. Scatter plot of $\overline{k}$ obtained from: differencing and high-pass filtering for random waves (*a*), ensemble averaging and high-pass filtering for regular waves (*b*), and differencing and high-pass filtering for regular waves (*c*). Slope of the best fit line and r^2 value shown on plot.

that the waves are repeatable. This conclusion is supported by the ensemble averaging estimate for the repeated random runs at P5.

The vertical variation of $\overline{k}$, shown in figure 5, was similar among all three methods, indicating that the structure of $\overline{k}$ was not affected by the method used to extract the turbulent signal. This is verified in figure 6, where scatter plots of $\overline{k}$ estimated using each method show that the three methods are linearly correlated in both the random and regular wave cases ($r^2 > 0.93$). Data from P3 were not included here because the high-pass filtering estimates were significantly biased by wave harmonics above 1 Hz at P3 due to the highly nonlinear waves near the onset of breaking.

7. Turbulence observations over the bar

7.1. Cross-shore and vertical variation of $\overline{k}$

Figure 7 shows the cross-shore and vertical variation of $\overline{k}$, where the estimates from ensemble averaging and differencing have been scaled to the high-pass filtering estimate using the ratios (slopes) given in figure 6 (i.e. for the random wave case, all differencing estimates were divided by 5.0). All three methods show the same vertical and cross-shore variation, which gives us confidence that the observed structure of $\overline{k}$ is accurate.

In the region where waves were breaking (P4–P6), estimates of $\overline{k}$ were largest near trough level and decayed

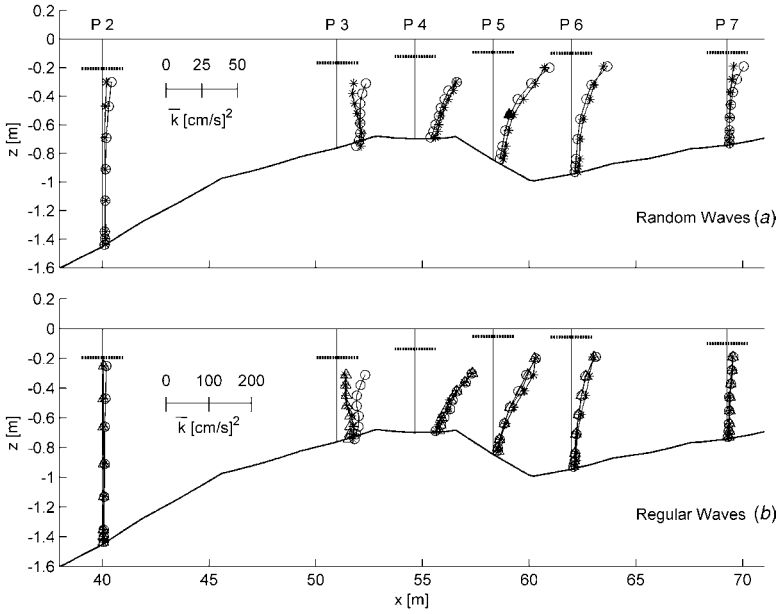

Figure 7. Cross-shore and vertical variation of $\overline{k}$ for the random (*a*) and regular (*b*) wave cases using ensemble averaging estimates divided by 4.2 (Δ), high-pass filtering estimates (○), and differencing estimates divided by 5.0 (random) and 5.3 (regular) (∗). Ensemble averaging estimate from the repeated random wave runs divided by 4.2 included at P5 (▲). Trough level indicated by (- - -).

with depth, as expected. Directly over the bar crest (P4), $\overline{k}$ was significant throughout the water column, even 1 cm above the bed. Interestingly, this seems to be a localized feature, as only a few metres onshore (P5), $\overline{k}$ was confined to the upper portion of the water column, a trend that continued onshore. Approximately 1.5 wavelengths onshore of the bar crest (P7) there was very little turbulence within the water column, consistent with observations that the waves had reformed at this location. Offshore of the bar crest (P3), estimates from the ensemble averaging and differencing techniques suggest that turbulence generated at P4 may have been advected offshore and confined to a region near the bottom. This is the only location where the maximum value of $\overline{k}$ was not near trough level. Offshore of breaking (P2) $\overline{k}$ was approximately zero and provides an indication of the noise level in our estimate of $\overline{k}$. Estimates from P1 were also near zero and not included in figure 7.

It is interesting to note that in the regular wave case, $\overline{k}$ estimated 1 cm above the bed was an order of magnitude larger at P4, where wave breaking was intense, than at P2 and P7, where the waves were not breaking. If the increase in $\overline{k}$ at P4 was due to boundary layer processes, we would expect it to be accompanied by a large change in the peak near bottom wave velocity. However, the peak wave velocity measured 1 cm above the bed at P4 was only 25% less than the velocity at P2 and 2% less than the velocity at P7, far from an order of magnitude change. This, along with the vertical variation of $\overline{k}$, suggests that the increase in near-bed turbulent kinetic energy at P4 was due to turbulence generated by breaking waves at the surface that was transported to the bed, and not bottom boundary layer processes.

Although the structure of the turbulence was similar for the random and regular wave cases, the magnitude of $\overline{k}$ was significantly smaller in the random wave case (approximately five times smaller at P4), despite similar offshore wave conditions. This is most likely due to inherent differences in the wave breaking properties for regular and random wave fields. For example, one reviewer noted that the surf zone created in the random wave case was broader than in the regular wave case. This allowed the wave energy to be dissipated within a larger volume of water and reduced the average turbulent energy observed at a fixed point in the water column. Additionally, the percentage of waves that broke over the bar was smaller in the random wave case because it contained waves that were small enough to propagate over the bar without breaking. A portion of the difference observed by George *et al* (1994) between scaled estimates of turbulence intensity obtained from laboratory tests using regular waves and field observations where random seas exist may be explained by the difference observed here in the random and regular wave cases along with the fact that different methods were used to separate the wave-induced and turbulent components of velocity in the lab and field tests.

7.2. *Local isotropy*

The isotropy of the turbulence was analysed in the region where large turbulent velocities were observed (P4, P5, P6—only elevations greater than 10 cm above the bed). Table 2 shows the ratio of the three components of the velocity variance to $2\overline{k}$ for the random and regular wave cases using all three separation methods. This indicates the relative importance of each component of the variance to $\overline{k}$. Values from other characteristic flows are provided as a reference (Svendsen 1987). From this table we see that the ensemble averaging and differencing methods consistently produced turbulence estimates that were not isotropic and were dominated by the cross-shore component of the variance ($\overline{u'u'}$). This is similar to a plane wake, but unlike a plane wake, the vertical component ($\overline{w'w'}$) was the least important. Estimates from the high-pass filtering method were not consistent with the other two methods, despite the similarities observed in the structure

Table 2. Isotropy of the average turbulence in the upper water column where wave breaking was observed. Values are the ratio of the average turbulent velocity variance to $2\overline{k}$, where the averaging is applied to all measurements greater than 10 cm above the bed. Data for other flows are from Svendsen (1987).

		P4			P5			P6		
	Method	$\overline{u'u'}$	$\overline{v'v'}$	$\overline{w'w'}$	$\overline{u'u'}$	$\overline{v'v'}$	$\overline{w'w'}$	$\overline{u'u'}$	$\overline{v'v'}$	$\overline{w'w'}$
Random	High-pass filter	0.40	0.30	0.30	0.36	0.32	0.32	0.35	0.31	0.34
	Ensemble average	–	–	–	0.38	0.34	0.28	–	–	–
	Differencing	0.48	0.31	0.21	0.45	0.32	0.23	0.46	0.29	0.25
Regular	High-pass filter	0.34	0.34	0.32	0.33	0.35	0.32	0.34	0.33	0.33
	Ensemble average	0.42	0.33	0.25	0.40	0.34	0.26	0.38	0.34	0.29
	Differencing	0.47	0.32	0.21	0.49	0.30	0.21	0.48	0.29	0.23
Other flows	Homogen. isotrop.	0.33	0.33	0.33						
	Plane wake	0.42	0.26	0.32						
	Bound layer (inner)	0.62	0.28	0.10						

of $\overline{k}$. This suggests relatively large anisotropy in the lower-frequency (less than 1 Hz) observed fluid motions compared to higher-frequency (greater than 1 Hz) fluid motions. The similarities observed between the ensemble averaging and differencing methods further indicate that these methods can be used to analyse the details of wave breaking turbulence. In every case, the near-bed turbulence (less than 10 cm above the bed) was anisotropic due to confinement of the vertical component of the variance by proximity to the bed.

8. Conclusions

Data obtained as part of a large-scale laboratory experiment to study the turbulence generated by waves breaking on a fixed barred beach were presented. This data set included synoptic measurements of the fluid velocity and free surface elevation for one random and one regular wave case. The fluid velocity was measured at seven locations within the cross-shore. At each location eight points were measured in the vertical direction, beginning 1 cm above the bed and extending to approximately trough level.

An analysis of the cross-shore and vertical variation of the time-averaged turbulent kinetic energy per unit mass ($\overline{k}$) showed that

1. Wave breaking turbulence was largest at the bar crest (P4) and influenced the entire water column, indicating that it may be important for near-bed processes on a barred beach, even in a time-averaged sense. Landward of the bar (P5, P6) the turbulence was confined to the upper layer and had dissipated once the waves reformed (approximately 1.5 wavelengths onshore of the bar crest, P7).
2. The cross-shore and vertical structure of the turbulence was similar in the random and regular wave cases. However, the magnitude of $\overline{k}$ in the regular wave case was as much as five times larger than the random case, despite similar offshore wave conditions.
3. The magnitude of $\overline{k}$ varied by as much as a factor of 5 based on the method used to separate the wave-induced and turbulent velocities, but the cross-shore and vertical structure of $\overline{k}$ was independent of the method used.
4. The differencing method proposed by Trowbridge (1998) appeared to be the most promising as it agreed closely with ensemble averaging and can be applied to random wave fields. This agreement was both in terms of the magnitude and structure of time-averaged quantities ($\overline{k}$ and isotropy), and in the signature of the time-dependent turbulent kinetic energy.

These observations are an important step toward understanding the dynamics of nearshore turbulence. Future work will be aimed at addressing not only the mechanisms responsible for the vertical and cross-shore transport of the turbulence generated by wave breaking, but also the contribution of shear production to the total turbulent energy within the surf zone and the rate of turbulent dissipation (e.g., Ting and Kirby (1995)). We plan to investigate the intermittency observed in k and the effect that intense wave breaking events have on velocities averaged over several wave periods. Our observations may also be used to aid in the development of numerical models aimed at predicting the detailed hydrodynamics of waves breaking over a barred beach.

Acknowledgments

This work was partially funded by the National Science Foundation under grants no. CMS-0086571, EEC-0244205, and OCE-0351741. The authors would like to thank Terry Dibble and Emi Fujii for their work in setting up and conducting the experiment as well as the valuable discussions with Dr Merrick Haller and Dr Tuba Özkan-Haller.

References

Battjes J A 1974 Surf similarity *Proc. 14th Int. Conf. on Coastal Eng.* (ASCE) pp 466–80

Bowen A J, Inman D L and Simmons V P 1968 Wave 'set-down' and 'set-up' *J. Geophys. Res.* **73** 2569–77

Cox D T and Kobayashi N 2000 Identification of intense, intermittent coherent motions under shoaling and breaking waves *J. Geophys. Res.* **105** 14223–36

Cox D T, Kobayashi N and Okayasu A 1995 Experimental and numerical modeling of surf zone hydrodynamics *Res. Report CACR-95–07 (PhD dissertation of first author)* Center for Applied Coastal Research, University of Delaware p 293

Elgar S, Raubenheimer B and Guza R T 2001 Current meter performance in the surf zone *J. Atmos. Ocean. Technol.* **18** 1735–46

Fredsøe J and Deigaard R 1992 *Mechanics of Coastal Sediment Transport* (Singapore: World Scientific) p 369

Garcez Faria A F G, Thornton E B, Lippmann T C and Stanton T P 2000 Undertow over a barred beach *J. Geophys. Res.* **105** 16999–7010

George R, Flick R E and Guza R T 1994 Observations of turbulence in the surf zone *J. Geophys. Res.* **99** 801–10
Goda Y 2000 *Random Seas and Design of Maritime Structures* 2nd edn (London: World Scientific) p 443
Goring D G and Nikora V I 2002 Despiking acoustic Doppler velocimeter data *J. Hydraul. Eng.* **128** 117–26
Hattori M and Aono T 1985 Experimental study on turbulence structures under spilling breakers *The Ocean Surface* ed Y Toba and H Mitsuyasu (Hingham, MA: Reidel) pp 419–24
Hoefel F and Elgar S 2003 Wave-induced sediment transport and sandbar migration *Science* **299** 1885–7
Jonsson I G 1966 Wave boundary layers and friction factors *Proc. 10th Int. Conf. on Coastal Eng.* ASCE) pp 127–48
Nadaoka K, Hino M and Koyano Y 1989 Structure of the turbulent flow field under breaking waves in the surf zone *J. Fluid Mech.* **204** 359–87
Nadaoka and Kondoh T 1982 Laboratory measurements of velocity field structure in the surf zone by LDV *Coast. Eng. Japan* **25** 125–46
Nikora V I and Goring D G 1998 ADV measurements of turbulence: can we improve their interpretation? *J. Hydraul. Eng.* **124** 630–4
Sancho F *et al* 2001 Wave hydrodynamics over a barred beach *Proc. Waves 2001* ASCE) pp 1170–9
Stive M J F 1980 Velocity and pressure field in spilling breakers *Proc. 17th Int. Conf. on Coastal Eng.* ASCE, 1 547–66
Stive M F and Wind H G 1982 A study of radiation stress and set-up in the nearshore region *Coast. Eng.* **6** 1–25
Svendsen I A 1987 Analysis of surf zone turbulence, *J. Geophys. Res.* **92** 5115–24
Thornton E B, Dalrymple R A, Drake T, Gallagher E, Guza R T, Hay A, Holman R A, Kaihatu J, Lippmann T C and Özkan-Haller T 2000 State of nearshore processes research: II *Technical Report NPS-OC-00-001* (Monterey, CA: Naval Postgraduate School) 37 pp
Ting F C K and Kirby J T 1994 Observation of undertow and turbulence in a laboratory surf zone *Coast. Eng.* **24** 51–80
Ting F C K and Kirby J T 1995 Dynamics of surf-zone turbulence in a strong plunging breaker *Coast. Eng.* **24** 177–204
Trowbridge J 1998 On a technique for measurement of turbulent shear stress in the presence of surface waves *J. Atmos. Ocean. Technol.* **15** 290–8
Trowbridge J and Elgar S 2001 Turbulence measurements in the surf zone *J. Phys. Oceanogr.* **31** 2403–17